Journal of Applied Automation Technologies

Research Paper

Cluster Consistency Constrained Informer Model for Long-Term Battery Health Prediction in Energy Storage Stations

Elżbieta Nowosad[1, *], Genowefa Pacholska[1] and Stefania Wioletta Gajewska[1]

[1] Faculty of Automation Technology, University of Applied Sciences in Pila, Pila, 64-920, Poland
*Corresponding author: elzbieta.n@wsz-pila.pl

Abstract. Numerous battery packs and clusters operating under different current, temperature, and ageing conditions are found in the energy storage systems. In these situations, the battery state-of-health's long-term deterioration and pack-to-pack variability must be taken into account for estimate. This research proposes a cluster-aware long-sequence Informer model for battery SOH estimation in energy storage facilities. The model includes degradation-stress sparse attention and consistency-constrained estimate after reconstructing degradation sequences from voltage, current, temperature, capacity, internal resistance, charge-discharge depth, and operational stress variables. The suggested model obtained 0.82% MAE, 1.17% RMSE, and 0.974 R^2 in experiments based on station-level battery operating data; concurrently, the cross-cluster SOH dispersion error was lowered by 23.6% in comparison to the conventional Informer. The findings demonstrate how long-sequence attention may increase SOH estimation accuracy under challenging energy storage operating settings and solve the issue of slow-degradation trends.

Keywords: *Battery Health Estimation, Cluster Consistency, Long-Sequence Informer, Degradation-Stress Attention*

Received on 07 July 2024, Accepted on 10 December 2024, Published on 17 December 2024

Introduction

The new energy storage facility will serve as a center for the utilisation of renewable energy, peak-shaving and frequency control services, power grid emergency supplies, and flexible-grid assistance. The health of the lithium-ion battery packs immediately affects the operating stability of these units; capacity fading, an increase in internal resistance, temperature irregularities, and cell imbalance all directly lower the available power and safety margin for dispatch. Battery State of Health may be used as a station-level operational parameter for economic scheduling and maintenance planning, as well as a laboratory deterioration index. Data-driven models may extract health-related information from voltage, current, temperature, and capacity sequences, according to recent research in deep learning for SOH estimate, digital battery management, and energy storage analysis [1]. Because station operation differs from controlled cycle testing, there are irregular charge-discharge curves, short rest intervals, frequent temperature fluctuations, and uneven battery module ageing. As a result, rather of being a standard regression work, the correct SOH estimation issue is an extended sequence learning problem [2].

Equivalent-circuit modelling, incremental capacity analysis, Gaussian process regression, ensemble learning, recurrent neural networks, convolutional networks, and hybrid deep learning models are some of the current techniques for estimating SOH. Although the methods have improved estimation accuracy for some particular datasets, there are still some issues with energy storage station applications. First, the gradual cumulative deterioration over hundreds of working cycles is not adequately captured by many models, which employ a brief window of recent voltage or current data [3]. Second, non-uniform ageing and balancing stress are not well-represented by pack-level and cluster-level inconsistency, which is frequently regarded as noise [4]. Third, unexpected temperature or current variations may result in overconfident health predictions since uncertainty and long-horizon drift are frequently overlooked [5]. Research on deep learning techniques and battery SOH estimate has also demonstrated that in real-world applications, models must be resilient to partial cycle data, changing operating circumstances, and disparate battery histories [6].

This research proposes a cluster-aware long-sequence Informer model for battery SOH estimation in energy storage facilities. The degradation path and group heterogeneity of extended operation are studied using the model. Utilise electrical, thermal, and capacity-related observations to reconstruct degradation-state features; apply a consistency-constrained SOH estimate aim to stabilise station-level prediction; and choose health-informative temporal segments using degradation-stress sparse attention. This study will address three technical issues: unstable SOH estimate under operational disturbance, poor modelling of cluster-level health dispersion, and a lack of representation for long-term battery deterioration. This research provides a workable learning framework for station-level battery health monitoring and lifecycle management by combining long-sequence attention with battery degradation stress indicators. A station-oriented estimating technique that connects SOH prediction with cluster consistency, operational stress, and BMS deployment needs is also expected, in addition to a small number of mistakes in the benchmark dataset.

Related Work

Station-Level Battery SOH Estimation

The goal of battery SOH estimate is to measure the reduction in capacity or power capability in comparison to the nominal condition. Energy storage station SOH estimate is useful for load balancing, safety analysis, capacity planning, and maintenance scheduling. The conventional techniques are often incremental capacity characteristics, equivalent-circuit parameters, impedance measurements, and offline capacity testing. These techniques are interpretable, but because full charge-discharge cycles are uncommon and grid dispatch dictates load profiles, they are not appropriate for continuous operation at the operating station. Thus, data-driven approaches are becoming common. The nonlinear deterioration properties of voltage, current, temperature, and capacity sequences may be learned using deep learning [7]. It has also been demonstrated that battery health indicators may be derived from real measurement signals using online SOH estimates based on frequency excitation, flexible energy storage data, and optimised ensemble learning [8]. Pack-level health assessment should take into account both individual cell behaviour and the overall operational condition, according to big data analysis of battery packs [9].

There are two ways that single-cell prediction and station-level SOH estimate are different. Hierarchy is the first. There are cells, modules, packs, clusters, and power conversion units in a station, and there is no direct correlation between the projected health of one level and another. Operating diversity is the second. Current sharing, thermal conditions, and equalisation histories will vary among clusters. Studies on energy storage frequency modulation have demonstrated that station operation can result in dynamic power needs and numerous shallow cycles, which can alter degradation stress [10]. According to battery management reports, the monitoring method should adjust to the real-world conditions of data availability and operation [11]. Thus, extended histories, incomplete cycles, cluster inconsistency, and dynamic stress characteristics should all be handled by an effective station-level SOH estimator within a single, cohesive framework [12]. Station employees in the first group are paid less. While an upper bound for the SOH estimate can result in a dispatch plan that the station is unable to execute, a lower bound will decrease the available capacity while still being safe. As a result, station-level health estimate should strive for a low average error while maintaining the relative order of cluster health and identifying aberrant dispersion before it becomes a capacity bottleneck.

Multi-Cell Consistency and Degradation Feature Modeling

Charging current, high temperature, prolonged depth of discharge, high current rate, lengthy rest periods, and cell irregularities all contribute to battery deterioration. Differential ageing is frequently caused by the various manufacturing methods, temperatures, and electrical loads of the individual cells in a multi-cell battery pack. The weakest cell or the most deteriorated module may restrict a pack's useful capacity, according to research on cell balance estimate and pack inconsistency [13]. There is an inconsistency issue at the pack level, according to reliable SOC estimate and balance evaluation studies [14]. The model will produce a smooth average health value and be unable to identify local degradation threats if SOH calculation ignores this. As a result, in addition to general voltage and current trends, the model of deterioration features should also take cell and cluster dispersion characteristics into account.

By examining voltage curve segments, incremental capacity peaks, charging time, temperature slope, and internal resistance proxies, machine learning techniques often construct health indicators. Uncertainty-aware estimations are obtained using Gaussian Process Regression and indirect health indicators, and the nonlinear mapping capacity is enhanced by optimised ensemble learning [15]. Although deep learning models like CNN, LSTM, encoder-decoder networks, and hybrid architectures minimise the need for human feature engineering, they still need physically significant input data in order to generalise under various operating situations [16]. Cumulative ampere-hour throughput, equivalent complete cycles, average temperature, temperature gradient, charge-discharge depth, voltage recovery, internal resistance fluctuation, and cluster-level dispersion are among the qualities that energy storage stations can offer. These are appropriate for long-sequence modelling because they involve both electrochemical ageing and stress brought on by station operation [17].

Additionally, research on pack-level neural estimating has demonstrated that special representation, as opposed to a single averaged feature vector, is needed for multi-series and multi-parallel battery topologies [18]. Local pack behaviour can uncover hidden discrepancies before the station-level average is anomalous, according to studies on abnormal battery localisation [19]. The inaccuracy under nonstationary battery operation may be decreased by merging statistical degradation models with deep learning, as demonstrated by hybrid SOH estimate and remaining usable life prediction techniques [20]. In order to learn station-level deterioration while maintaining the health disparities within clusters, this research will employ cluster-aware sequence encoding based on the results [21].

Long-Sequence Attention Models for Health Prognostics

Because deterioration under operational stress progresses slowly and responds slowly, long-sequence time-series forecasting has been gradually used to battery health management. Although they can lose distant information in lengthy sequences, recurrent models solve the issue of time dependency. Although temporal convolution uses dilation to increase the receptive field, its fixed kernels are less appropriate for erratic station functioning. Although complete attention is computationally costly, transformer-based models can use attention to link distant time steps. In order to solve the issue of long-term monitoring data, Informer lowers this cost using ProbSparse attention and sequence distillation [22]. Sparse attention can retain important temporal information by not giving all redundant points identical weight, as demonstrated by Informer and other long-sequence forecasting experiments [23].

Additionally, battery health prognostics require robustness and uncertainty management. Studies on remaining usable life indicate that combining sequence learning with degradation-sensitive indicators improves long-term degradation predictions [24]. Bayesian deep learning has been used to quantify the uncertainty in SOH estimation for lithium-ion batteries. The modelling of long-range dependencies for battery management is anticipated to be improved, and transformer-based battery state estimate has begun to emerge in recent research [25]. Because battery deterioration is not a universal signal, it is not possible to directly apply the general Informer to station-level SOH estimate. Pack irregularity, temperature history, and cumulative stress are the causes. Consequently, cluster-aware embedding, degradation-stress attention, and consistency requirements need be included into a battery-oriented long-sequence Informer [26].

The need for long-context models has been reinforced by recent studies in deep learning reviews, Transformer-based state estimates, and battery monitoring sensors. Although SOH estimation is more reliant on delayed deterioration memory and past stress buildup, transformer observers can enhance the depiction of nonlinear SOC dynamics [27]. Effective battery monitoring models have also demonstrated that realistic health assessment should take data availability and implementation costs into account in addition to offline accuracy [28]. Future research on deep learning-based battery state estimation will likely concentrate on strengthening robustness, improving feature interpretability, and boosting adaptability to real-world operating situations [29]. Physically relevant health markers remain beneficial even when a neural network model is employed, according to control-oriented investigations of cyclable lithium estimate [30]. Therefore, rather of relying solely on latent attention weights, the suggested approach maintains degradation stress and cluster dispersion as explicit inputs.

Cluster-Aware Long-Sequence Informer Model

Cluster-Aware Degradation Sequence Encoding

At the station level, a few battery clusters will be observed. Voltage data, current profile, temperature statistics, capacity-related indications, charge-discharge depth, internal resistance proxy, cumulative throughput, and balancing status are all available at each time step. Instead of acquiring the degradation sequence directly from the raw signal, the model generates a time-dependent and cluster-inconsistent degradation sequence. The cluster-aware long-sequence Informer architecture shown in Figure 1 transforms BMS data into degradation-state embeddings, applies sparse attention processing, makes corrections using consistency constraints, and then provides SOH estimates.

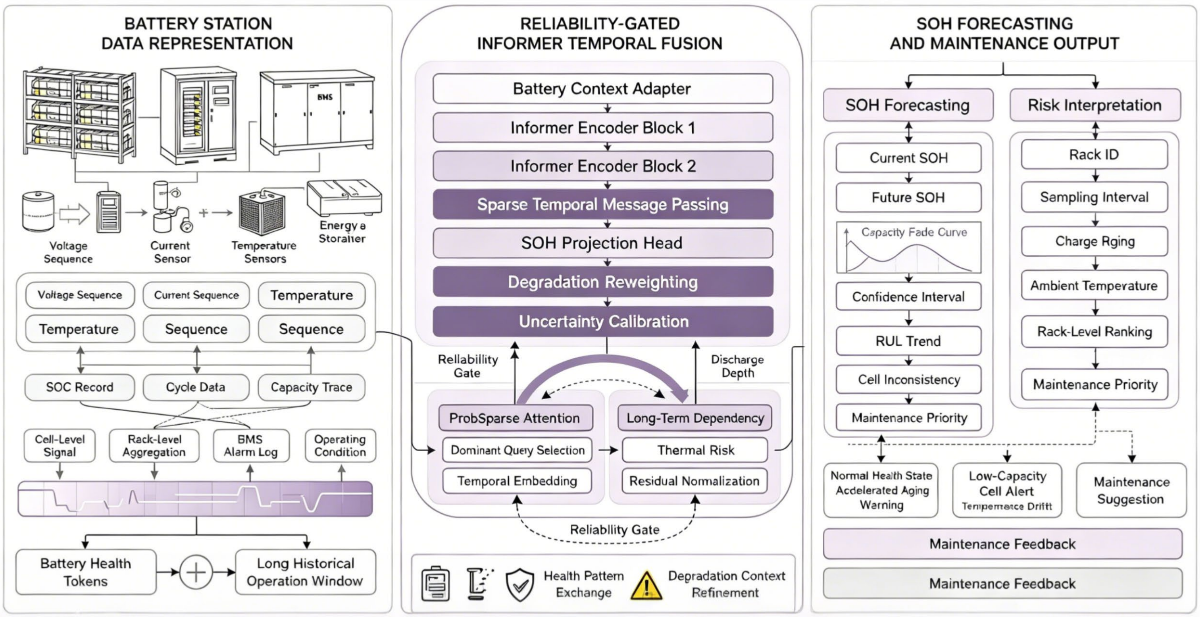

Figure 1. Cluster-aware long-sequence Informer framework for station-level SOH estimation

For the c -th battery cluster at time t, the raw measurement vector is denoted by $x_{t,c}$. A degradation-state vector is constructed by combining instantaneous measurements, temporal increments, cumulative stress, and cluster dispersion.

$$r_{t,c} = W_r\left[x_{t,c} \oplus \Delta x_{t,c} \oplus s_{t,c} \oplus d_{t,c}\right] \quad \text{Eq.(1)}$$

where $s_{t,c}$ represents cumulative degradation stress and $d_{t,c}$ denotes cluster-level dispersion features. This representation prevents the estimator from relying only on recent voltage or temperature values and makes long-term operating stress visible to the sequence model. In station data, one cluster may experience higher thermal exposure during the same dispatch command because of cabinet airflow or pack location. The reconstructed state therefore preserves cluster-specific degradation causes instead of forcing all clusters into one shared average trajectory.

$$s_{t,c} = \alpha Q_{t,c} + \beta DOD_{t,c} + \gamma T_{t,c}^{avg} + \delta R_{t,c} \quad \text{Eq.(2)}$$

The stress term contains accumulated charge throughput $Q_{t,c}$, depth of discharge $DOD_{t,c}$ average temperature $T_{t,c}^{avg}$, and internal resistance proxy $R_{t,c}$. The coefficients are learnable and constrained to be non-negative, so that stronger operating stress cannot reduce the degradation representation. This constraint is useful in practice because a purely unconstrained neural layer may fit short-term measurement noise and produce physically inconsistent health embeddings.

$$d_{t,c} = \left|x_{t,c} - \mathrm{mean}_c(x_{t,c})\right| + std_c(x_{t,c}) \quad \text{Eq.(3)}$$

Cluster dispersion is calculated from the deviation between one cluster and the station-level mean, together with crosscluster standard deviation. This term is important because an energy storage station may show acceptable average health while one cluster ages faster than others.

$$e_{t,c} = r_{t,c} + P^t(t) + P^c(c) + P^o(o_t) \qquad \text{Eq.(4)}$$

The final embedding $e_{t,c}$ includes temporal position, cluster identity, and operation-mode embedding $P^o(o_t)$. Operation mode distinguishes charging, discharging, floating, and rest states, which helps the model interpret the same current or voltage pattern under different station actions.

Degradation-Stress Sparse Attention Mechanism

To simulate health reliance across a lengthy operational history, a long-sequence Informer backbone is used. Because there are several steady periods in the station data where SOH varies slowly, full attention is ineffective. Time steps containing stronger ageing information, such as high temperature, high current fluctuation, deep discharge, or aberrant cluster dispersion, are given greater weight in the suggested degradation-stress sparse attention.

$$a_{ij} = \frac{q_i^T k_j}{\sqrt{d}} + \lambda_1 s_j + \lambda_2 d_j \qquad \text{Eq.(5)}$$

The attention score a_{ij} combines query-key similarity with degradation stress s_j and dispersion d_j. This makes the model focus on health-informative periods rather than uniformly attending to all historical samples.

$$M_i = \max_j(a_{ij}) - \frac{1}{L}\sum_j a_{ij} \qquad \text{Eq.(6)}$$

The sparse query measurement M_i evaluates whether a query has a concentrated attention distribution. Queries with larger M_i are retained for exact attention, while low-information queries are approximated.

$$u = \lceil \kappa \ln(L) + \eta C \rceil \qquad \text{Eq.(7)}$$

The number of retained queries u depends on sequence length L and cluster count C. In the experiment, κ is set to 3.0 and η is set to 0.5, allowing the model to increase sparse-query capacity when more clusters are monitored.

$$H' = \mathrm{softmax}(A_u)V_u + \mathrm{mean}(V_{\neg u}) \qquad \text{Eq.(8)}$$

The selected attention output uses high-contribution values V_u and a residual mean term from unselected values. The residual term preserves slow health background and avoids losing weak but persistent degradation signals.

$$Z_l = \mathrm{Conv}_3(H_l) + \mathrm{Pool}_2(H_l) + H_l \qquad \text{Eq.(9)}$$

Temporal distillation compresses redundant long sequences through convolution, pooling, and residual transfer. After two distillation layers, a 720 -step input sequence is compressed to 180 hidden states, reducing memory cost while retaining long-term degradation patterns.

Consistency-Constrained SOH Estimation Objective

Cells are packed, clustered, and given SOH values by the decoder. The estimating head uses projection layers that are particular to the hierarchy and shares the long-sequence latent representation. The degradation-stress attention and cluster-consistency estimation module are displayed in Figure 2. In order to preserve consistency with the cell-level health dispersion, the consistency branch limits the pack and cluster estimates.

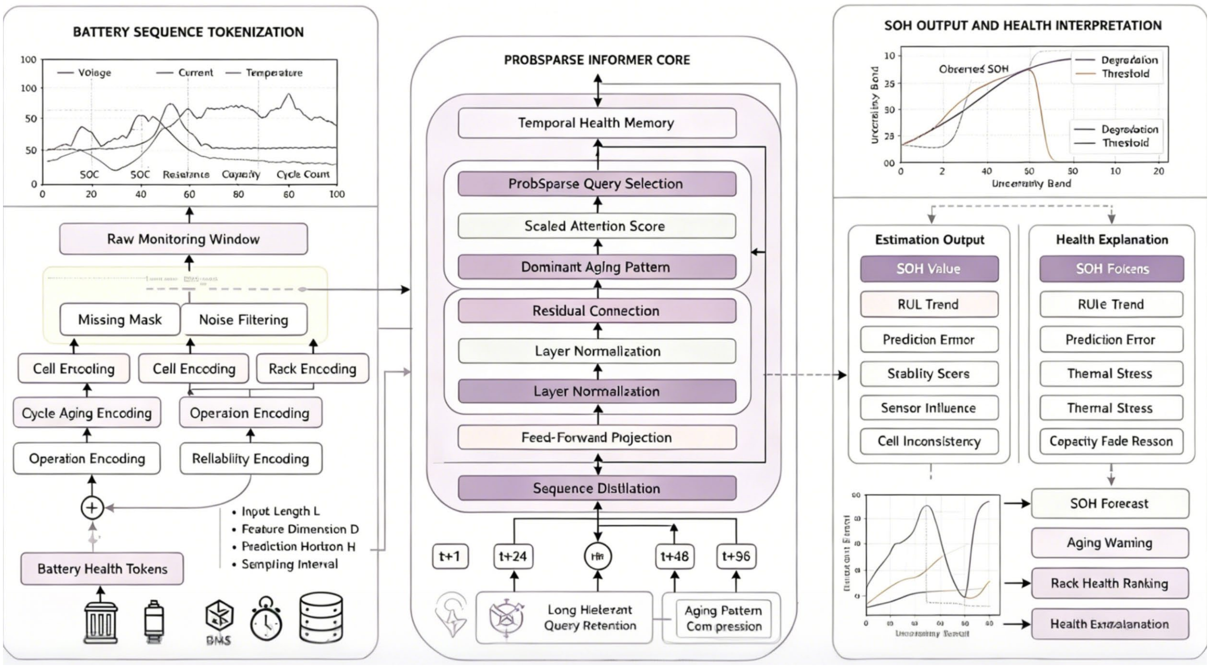

Figure 2. Degradation-stress attention and cluster-consistency estimation module

$$\hat{y}_{t,c}^{SOH} = W_h\left[z_{t,c} \oplus s_{t,c} \oplus d_{t,c}\right] + b_h \qquad \text{Eq.(10)}$$

The estimated SOH is generated from latent sequence state $z_{t,c}$, stress feature, and dispersion feature. This design allows one cluster to have a different health trajectory even when station-level operation commands are shared.

$$L_e = \sum_c \omega_c \left| y_{t,c}^{SOH} - \hat{y}_{t,c}^{SOH} \right| \qquad \text{Eq.(11)}$$

The estimation loss is a weighted absolute error. The weight ω_c is larger for clusters with stronger degradation dispersion, so the model pays more attention to clusters that may limit station capacity.

$$L_k = \left| std_c\left(\hat{y}_{t,c}^{SOH}\right) - std_c\left(y_{t,c}^{SOH}\right) \right| \qquad \text{Eq.(12)}$$

The consistency loss controls cross-cluster health dispersion. It prevents the model from producing overly smoothed estimates that underestimate pack inconsistency.

$$L_m = \max\left(0, \hat{y}_{t+\tau,c}^{SOH} - \hat{y}_{t,c}^{SOH} + \varepsilon\right) \qquad \text{Eq.(13)}$$

The monotonic degradation penalty discourages unrealistic SOH recovery over long horizons. A small tolerance ε is retained because measurement noise and calibration correction may produce slight apparent recovery.

$$L = L_e + \mu L_k + \nu L_m + \zeta \|\Theta\|_2^2 \qquad \text{Eq.(14)}$$

The final training objective combines estimation accuracy, cluster consistency, monotonic degradation regularization, and model weight penalty. In the reported setting, $\mu = 0.35, \nu = 0.20$, and $\zeta = 0.0001$. These values were selected on the validation set to balance accuracy, dispersion preservation, and smooth degradation behaviour across clusters.

Experimental Design and Quantitative Evaluation

Station-Level Battery Dataset and Cluster Configuration

An experimental dataset was generated using data from a lithium-ion energy storage system with 12 battery clusters, 96 packs, and 1,536 monitored cell groups. The monitoring period will span the first eighteen months from startup, with a five-minute sample interval. Cluster voltage, pack voltage, current, maximum and minimum cell voltage, temperature data, current-rate indication, cumulative ampere-hour throughput, energy throughput, charge-discharge mode, and BMS balance flag are among the accessible variables. Monthly SOH labels were created using laboratory capacity calibration data, and interim labels were interpolated using the calibrated deterioration curve. After removing duplicate timestamps and unusual communication records, 1.84 million valid monitoring samples remained. To train for 70%, validate for 15%, and test for 15%, time splitting was used. If the split had been random, the error values would have been too tiny and the future deterioration state would have seeped into the training set. The final test period encompassed both the standard dispatch day and a few high-power response windows, and all clusters maintained their initial time order. Instead of interpolating among comparable nearby samples, this design will allow the assessment to ascertain if the model can infer health decline from prior operations.

Three disturbance subgroups were maintained in order to replicate real-station conditions: shallow-cycle operation with a depth of discharge below 25%, high-temperature operation over 35°C, and high-current fluctuation surpassing 0.8C equivalent rate. The training procedure encompassed 60 hours of monitoring history and consisted of 720 stages. A larger window was chosen because, according to the preliminary research, the SOH-related stress indicators showed greater stability over a longer time span than those in a brief charge-discharge cycle. Longer missing periods were flagged with a reliability flag and omitted from calibration label alignment, whereas missing values less than 15 minutes were interpolated. The test set comprises both moderate deterioration periods and accelerated ageing periods since the dataset also includes high-temperature summer operation and low-temperature winter operation. Consequently, compared to a randomly shuffled battery cycling dataset, this arrangement will be more representative of the real conditions of a power plant. In order to avoid utilising the times just after cell replacement as the deterioration samples, the calibration labels have also been cross-referenced with the anomalous maintenance data. During this period, SOH will experience short-term recovery, and long-term learning may be complicated if the monotonic deterioration assumption is broken. The experiment can maintain the health trend more in line with typical station ageing by segmenting into maintenance-excluded sections.

Baseline Models and Health Estimation Indicators

Support Vector Regression, Random Forest, XGBoost, LSTM, GRU, TCN, Transformer, and the conventional Informer were compared to the suggested model. Convolutional temporal models, recurrent neural networks, attention-based long-sequence forecasting, and conventional machine learning are the basic models mentioned above. The same splits were used to train, verify, and test each deep model. Utilising training set statistics, standardise the input variables and represent SOH labels as a percentage of calibrated nominal capacity. MAE, RMSE, MAPE, R2, maximum absolute error, cluster dispersion error, long-horizon drift, inference delay, and parameter count are the evaluation indices. RMSE is used to raise the penalty for greater health variations that might result in poor maintenance choices, whereas MAE is used to measure the average station-level estimation error. The anticipated health distribution in clusters was compared to the calibrated data using cluster dispersion error. The models might not be able to detect a weak cluster if the average SOH error is not modest enough.

The whole-model fit is represented by R2, whereas MAE and RMSE are average errors. Whether the model preserves the cross-cluster health disparities is shown by the cluster dispersion error. To ascertain if the anticipated SOH trajectory would be comparatively stable under gradual deterioration, long-horizon drift is calculated within a rolling window of thirty days. Inference latency was measured on a CPU-only edge gateway and an industrial workstation with a single mid-range GPU. Only when a model's estimation accuracy and latency satisfy the BMS monitoring requirements will it be deemed station-deployable. Analyse how well the model preserves the evaluation record's cluster degradation order. Instead of addressing the full maintenance group, this directive focuses on the most damaged portion of the group. A model is essentially worthless if it has a low MAE yet reverses the health ranking of two clusters. As a result, ranking consistency, dispersion preservation, and trajectory smoothness are considered further proof of practical reliability during the validation process.

Training Strategy and Validation Protocol

An initial learning rate of 0.0006, a batch size of 24, a weight decay of 0.0001, and early halting for 15 epochs were all established, and AdamW was chosen as the optimiser. There are four attention heads, three encoder depths, and 128 hidden dimensions. The dropout rate is 0.08. The residual background coefficient (ρ) was 0.10

https://doi.org/10.64972/jaat.2024v2.345p37e:511-526

while the sparse-query coefficient (κ) was 3.0. To stop the chosen model from optimising just the station average, validation loss combines SOH estimation error with cluster dispersion error.

To validate robustness, three stress tests were created. In the first experiment, a temperature offset of ±3 °C was introduced, and the change was measured. Random current noise with a 5% standard deviation of the rated current was applied in the second test. In the third test, a communication problem was simulated and the sequence was shortened by 10%. Additionally, cross-cluster transfer was verified by first training on eight clusters and then testing on four new clusters after fine-tuning using 20% of their history data. Using this protocol, make sure the model has learnt deterioration patterns rather than just memorised cluster identities. If the model underestimates the weakest cluster, a tiny average MAE might be deceptive. Instead, note the prediction variance of the clusters in the validation set. When deploying a BMS, the estimator should be both smooth enough for capacity scheduling and conservative enough to reveal cluster inconsistency.

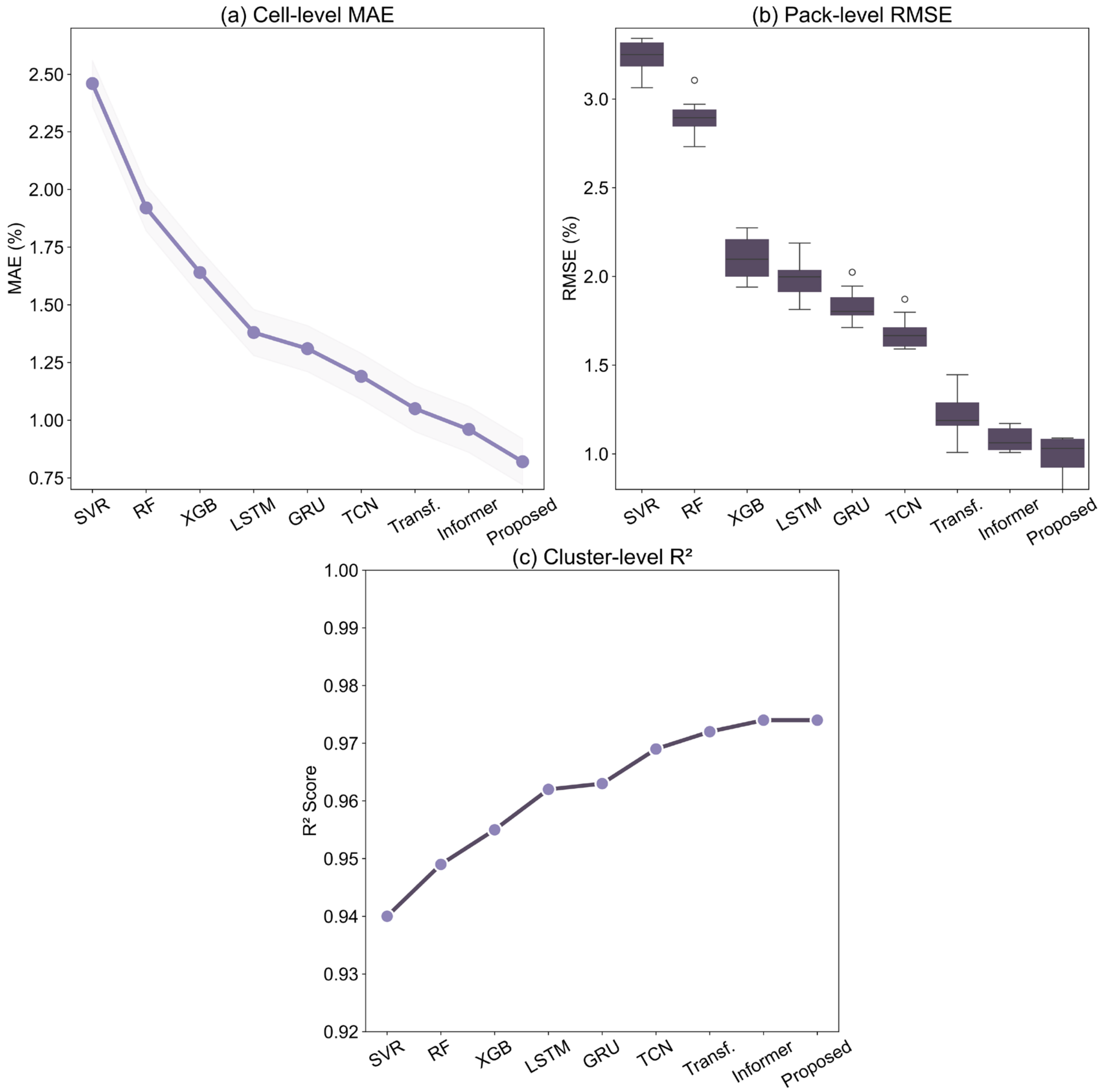

Figure 3. SOH estimation accuracy across battery hierarchies. (a) Cell-level MAE. (b) Pack-level RMSE. (c) Cluster-level R2.

https://doi.org/10.64972/jaat.2024v2.345p37e:511-526

Result Analysis and Operational Discussion

SOH Estimation Accuracy Across Battery Hierarchies

The novel cluster-aware Informer has been shown to have the highest accuracy of all the techniques based on the outcomes of the studies. Before determining the absolute error, look at the battery hierarchy's error distribution. Station dispatch capacity is determined by cluster-level estimates, pack-level estimates are impacted by module aggregation, and cell-level estimates are more vulnerable to local measurement noise. For station-level health management, a model that works well at one level is nonetheless inappropriate. Random forest lowers the MAE to 1.92%, whereas SVR achieves an MAE of 2.46% and an RMSE of 3.18%. Although XGBoost reaches an MAE of 1.64%, it has a greater inaccuracy when there is a substantial variation [31]. With an MAE of 1.38% and 1.31%, respectively, LSTM and GRU are able to capture temporal information in battery health assessment [32]. By using dilated convolutions to capture medium-range deterioration patterns, TCN further lowers MAE to 1.19% [33]. Standard Transformer costs more for memory but has a lower MAE of 1.05%. The suggested model has an MAE of 0.82%, an RMSE of 1.17%, an R2 of 0.974, and a maximum absolute error of 2.86%, whereas Standard Informer has an MAE of 0.96%. The battery hierarchy's SOH estimate accuracy is displayed in Figure 3. Cell-level MAE is shown in Figure 3(a), pack-level RMSE is shown in Figure 3(b), and cluster-level R^2 is shown in Figure 3(c). Because the suggested embedding precisely simulates the dispersion between clusters, the increase is comparatively greater at the cluster level. Thus, the primary engineering output to assist station scheduling will be the cluster-level result in this study. Cluster-level forecasts provide useable capacity and dispatch confidence, pack-level predictions facilitate maintenance localisation, and cell-level predictions provide diagnostic granularity. The novel method improves all three tiers and eliminates the necessity for the long-sequence representation to be at a single aggregate level.

A station-level average SOH would not accurately represent a local degradation risk; hence cluster consistency was also taken into account. The cluster consistency and health dispersion study are shown in Figure 4. The cluster SOH deviation is displayed in Figure 4(a), the pack inconsistency index is displayed in Figure 4(b), and the health dispersion trend over the test period is displayed in Figure 4(c). The suggested model lowers this bias to 5.4%, whereas the conventional Informer underestimates the cluster dispersion by 18.9%. Consequently, the consistency requirement allows for various health statuses among the clusters rather than requiring all clusters to have the same value. This is necessary for maintenance to prevent a weak cluster from limiting the energy storage station's overall discharge capacity [34]. Compared to the station-average SOH alone, the cluster dispersion curve is more operationally practical. Before the station's capacity drastically decreases, a balancing inspection or a cabinet-level thermal diagnosis can be scheduled if the dispersion is quite big and the average SOH is likewise high.

Degradation Trend Tracking and Disturbance Robustness

Used a 30-day rolling forecast window to assess the long-term trend monitoring. Compared to a single-point SOH estimation, the test is more rigorous, and even a slight daily bias will cause a notable variation in the health trajectory. The BMS may mistakenly identify a drift in the energy storage operating value as low residual capacity or delayed balancing. Consequently, rather of focusing just on the final test MAE, both the trajectory's form and the residuals' distribution were investigated. Our suggested model yielded a SOH curve that was marginally higher than the calibrated capacity record. The long-term deterioration trend tracking performance is shown in Figure 5. The distribution of residuals is shown in Figure 5(c), long-horizon drift is depicted in Figure 5(b), and SOH trajectory fitting is shown in Figure 5(a). The drift values for LSTM, TCN, Transformer, and conventional Informer are 0.86%, 0.71%, 0.63, and 0.55, respectively, whereas the suggested model decreases 30-day drift to 0.41%. 92.3% of the test samples fall within $pm 1.5%$ SOH error, indicating a smaller residual distribution for the suggested model [35]. This stability is mostly due to the fact that degradation-stress attention does not regard all history equally and instead chooses times with high information content, such as high temperature, deep discharge, and irregular dispersion. The identical outcome may be obtained by using the residuals' distribution. The baseline model overestimates SOH in accelerated ageing due to its larger positive tail. Capacity derating and thermal inspection may be delayed as a result of these energy storage management problems, which are more serious than small underestimates. The suggested model reduces the positive tail by using monotonic regularisation and stress-aware attention.

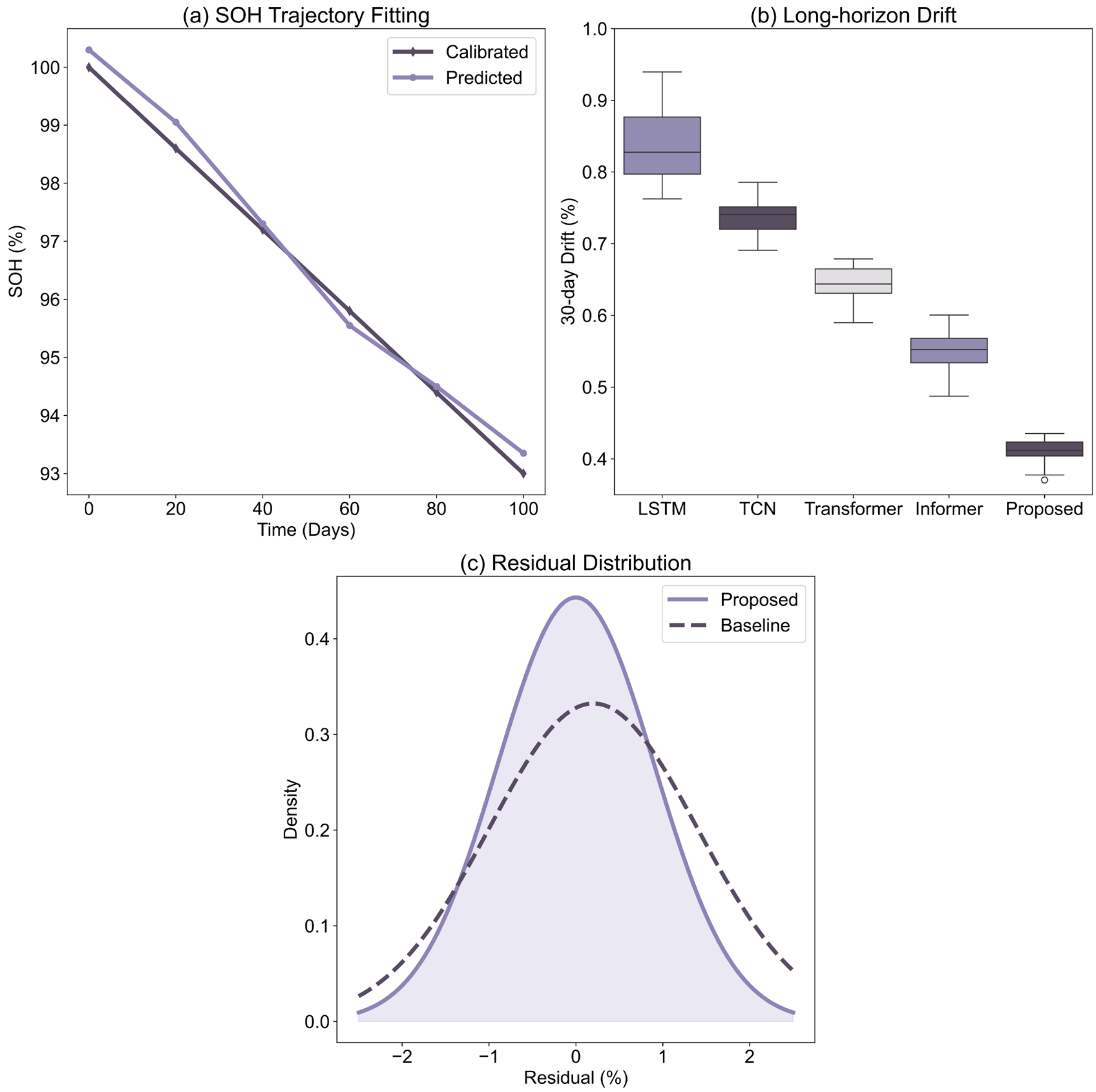

Figure 5. Long-term degradation trend tracking performance. (a) SOH trajectory fitting. (b) Long-horizon drift. (c) Residual distribution.

When stationarity-breaking factors are present, the model is rather stable. Both the MAE and the LSTM rise with a temperature offset of ±3 °C; the new values are 0.94% and 1.71%, respectively, from the original 0.82% and 1.38%. The typical Transformer has an R2 of 0.931, whereas the suggested model has attained 0.957 with the present noise. Using residual background attention and cluster-aware embedding, the model obtained an MAE of 1.05% with less than 10% missing sequence pieces [36]. As a result, some mistakes in the real BMS data can be handled by the model. Because cumulative throughput and dispersion properties can make up for the absence of complete charge-discharge cycle information, the model is more resilient to shallow-cycle operation [37]. For frequency regulation stations, the situation is different; many days have fragmented and shallow cycles. In these conditions, long-sequence stress buildup still indicates age-related decrease, although direct capacity-feature extraction is minimal. The suggested attention mechanism lessens the SOH trajectory's susceptibility to repeated low-information samples by giving greater weight to the few intervals with significant deterioration evidence.

Ablation, Transferability, and Deployment Analysis

To determine the reason behind the module failure, ablation tests were conducted. Any variations were caused by the model structure rather than the training schedule because the ablation versions employed the same optimiser, input length, and validation split during training. Cluster embedding, temporal distillation, consistency-constrained loss, and degradation-stress correction in attention were the four variations that were assessed. This architecture includes health-distribution control, computational compression, representation separation, and attention selection. The station hierarchy was considered important since the MAE rose from 0.82% to 1.01% in the absence of cluster embedding. The long-horizon drift rises from 0.41% to 0.59% when degradation-stress attention is removed. The biggest cluster dispersion error, which increases from 5.4% to 14.7%, happens in the absence of consistency loss. The ablation results of the consistency and attention restrictions are displayed in Figure 6. The module contribution is shown in Figure 6(a), parameters and FLOPs are displayed in Figure 6(b), and inference latency is compared in Figure 6(c). The suggested model has better SOH accuracy and is smaller than the whole Transformer, with 3.18 million parameters and 0.74 GFLOPs [38]. The modules' varying degrees are also demonstrated by the ablation findings. Consistency loss lessens health dispersion bias, degradation-stress attention improves long-horizon stability, and cluster embedding mainly increases pack and cluster accuracy. We can further appreciate why this approach works better than adding a general attention module to a battery data set by looking at the above split of functions. The latter work will be easier to modify. Strengthen temporal distillation if a station has limited processing power; give the consistency term more weight if cluster imbalance is the primary danger; and update the stress-attention term more often if the present profile changes frequently.

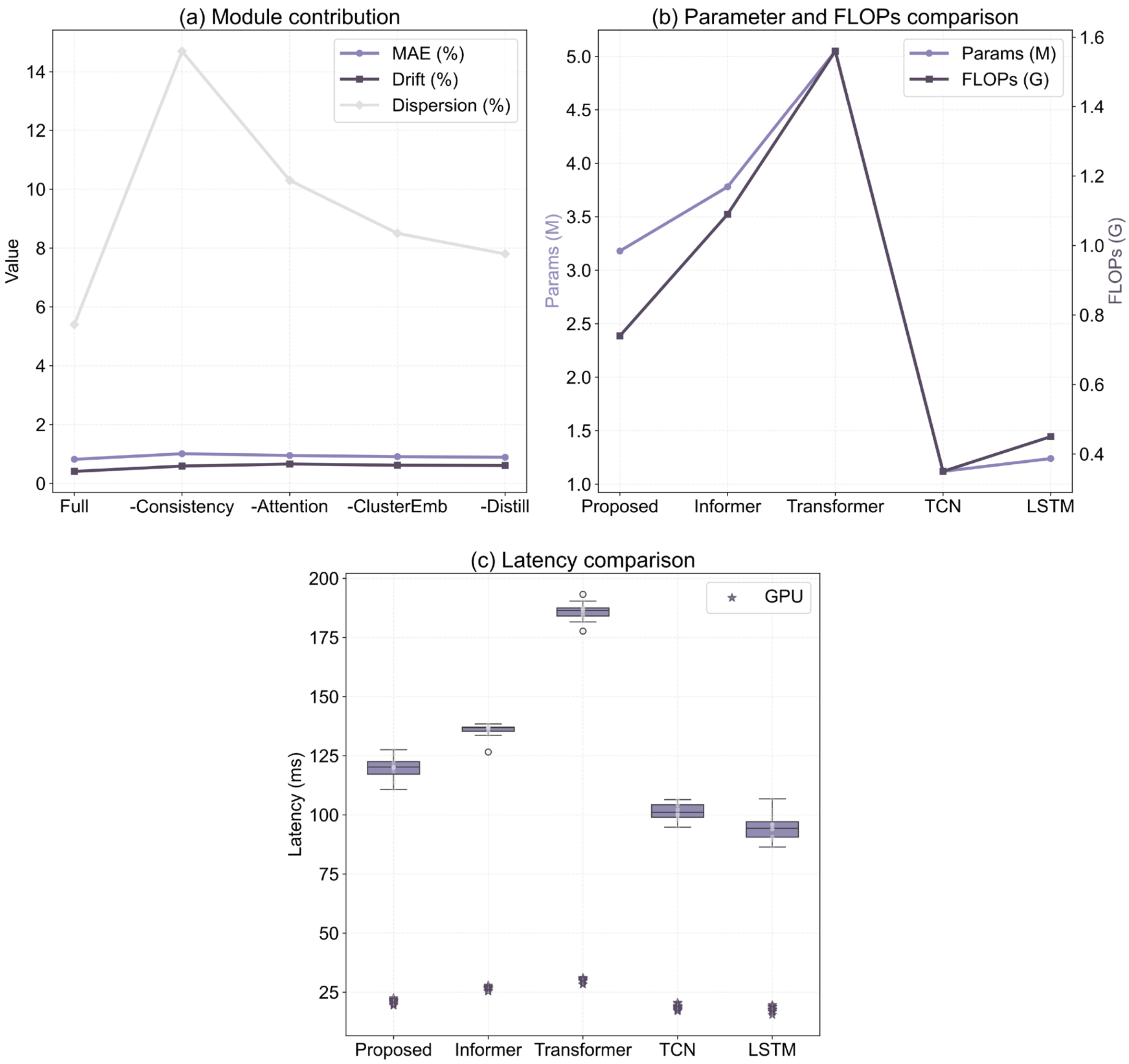

Figure 6. Ablation analysis of attention and consistency constraints. (a) Module contribution. (b) Parameter and FLOPs comparison. (c) Latency comparison.

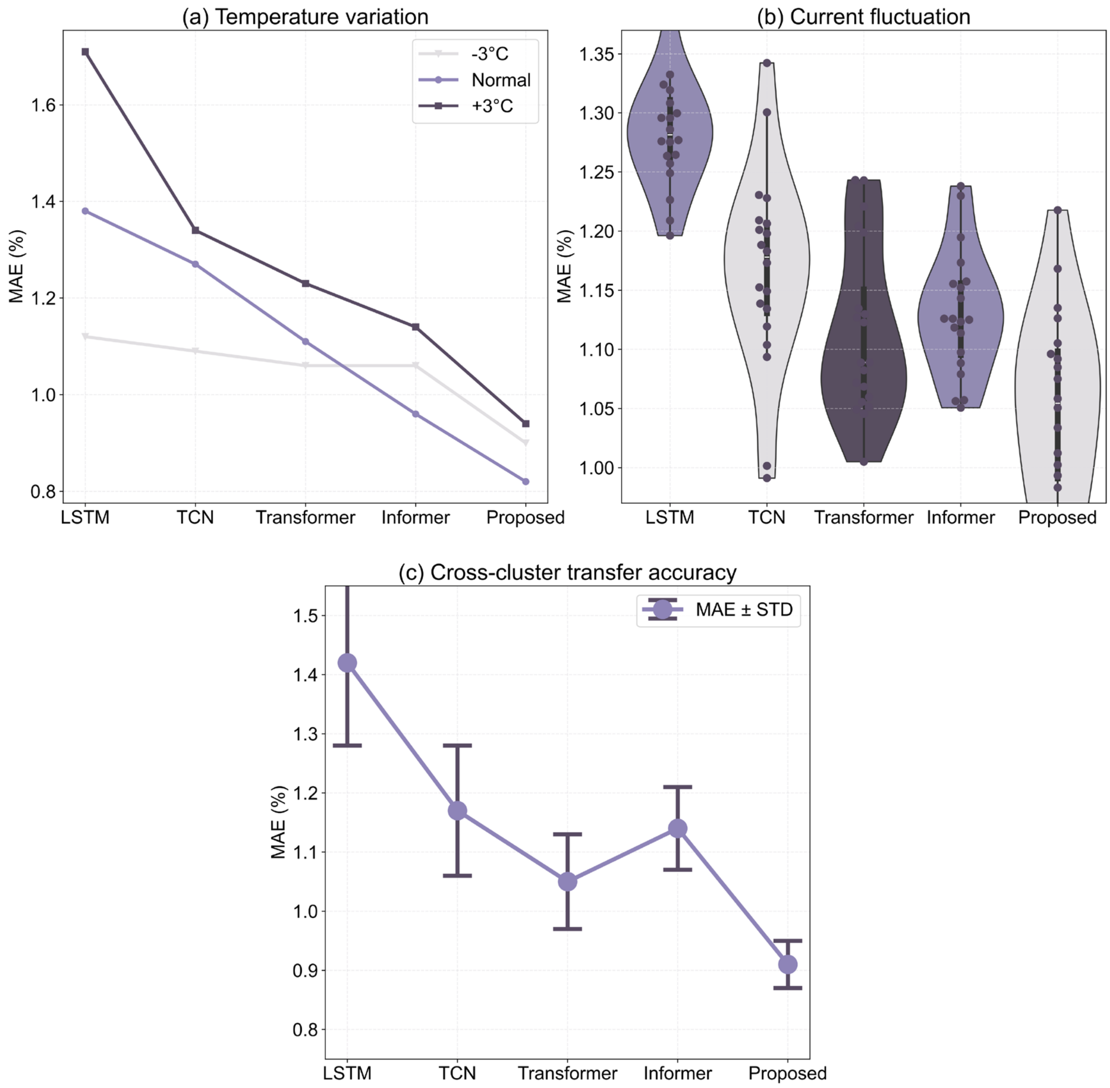

Figure 7. Robustness and cross-cluster transfer results. (a) Temperature variation. (b) Current fluctuation. (c) Cross-cluster transfer accuracy.

Figure 7 displays the outcomes of cross-cluster transfer. The performance variation with temperature is depicted in Figure 7(a), the stability under current fluctuation is shown in Figure 7(b), and the cross-cluster transfer accuracy is reported in Figure 7(c). The suggested model attains an MAE of 0.91% and the standard Informer is 1.14% after training on eight clusters and fine-tuning using 20% of the data from the unseen clusters. As a result, rather than only memorising cluster identifiers, the model has learnt to identify a general deterioration pattern [39]. Additionally, the transfer findings demonstrate the technical applicability of the suggested stress embedding. The accuracy could not be restored by fine-tuning using a little quantity of unseen-cluster data if the model simply employed the cluster labels. As an alternative, the model's correlations between throughput, temperature, current variation, dispersion, and SOH decrease can be reused, and the cluster embedding can then be modified to fit a different local degradation baseline. At the industrial workstation, the average inference delay for a station window is 21.6 ms. The CPU-only edge gateway does not have to adhere to the 5-minute sample interval requirement; its latency is 118 ms. As a result, the model may be incorporated into station-level BMS analytics, because SOH estimate requires stability and traceability over an extended period of operation rather than millisecond reaction [40]. The estimator will present a health trend chart for maintenance planning, initiate an energy management platform cluster-level dispersion alarm, and update the health status on a regular basis during real operation. If there has been a long-term drift in the cause of battery replacement or cabinet maintenance, the above procedure can be utilised to re-calibrate on a periodic basis during the monthly capacity test. This method can also be further lowered, according on the deployment study. Model pruning or low-bit quantisation may be used without changing the health-estimation logic as sparse attention already minimises unnecessary temporal processing. It is suitable for older station controllers that have comparatively extended monitoring durations but less processing capacity.

Conclusion

This research developed a cluster-aware long-sequence Informer model for battery SOH estimation in energy storage facilities. The model is based on the real-world observation that long-term operational stress and cluster-level inconsistency interact to produce the station-level SOH, which does not follow a single smooth deterioration curve. Long-term health dependencies are simulated using degradation-stress sparse attention, and a technique for reconstructing degradation sequences based on electrical, thermal, capacity-related, and cluster-dispersion data is shown. Because it preserves the accumulated stress information and differentiates between various cluster ageing phases, the new framework is better suited for station operation data than the short-window approach.

According to the trials, the new model has increased deployment efficiency, resilience, long-term stability, cluster consistency, and SOH estimate accuracy. The first is that it lowers the distribution's spread and mean error, which are typically not optimised at the same time. In comparison to the conventional Informer and recurring baselines, the model's 0.82% MAE, 1.17% RMSE, and 0.974 R^2 decreased cross-cluster dispersion bias. The reliability of station-level health assessment has been found to be enhanced by cluster embedding, consistency-constrained loss, and degradation-stress attention, according to ablation experiments.

The suggested architecture can be expanded in the future to incorporate online adaptation under seasonal operating variations, thermal safety margins, and electrochemical previous restrictions. For a high-risk SOH estimate, the operating margin can be increased by adding an uncertainty-aware alert threshold. compatible with digital twin systems and BMS edge devices for real-time capacity analysis and lifecycle maintenance planning. More stations, other mixed-battery chemistries, and long-term field degradation data will be used in future research to assess the model. Linking dispatch optimisation with SOH estimate is another excellent approach; in this way, the cluster's power allocation may be influenced by the anticipated health state. A cluster's power management system will lessen the load on it and transfer part of it to healthy clusters if it shows signs of deterioration. By using health estimation in a closed-loop manner, SOH prediction would become an active life-cycle management tool rather than a passive observation mode. In order to link data-driven SOH estimate with economical operation and safety-oriented asset management, the same architecture may be utilised to enable health-aware grouping, cluster rotation, and early replacement planning for big stations.

Author Contributions

Elżbieta Nowosad contributes to conceptualization, methodology, software, validation, analysis, investigation, data collection, draft preparation, manuscript editing, visualization, supervision. Genowefa Pacholska contributes to methodology, software, validation. Stefania Wioletta Gajewska contributes to analysis, investigation, data collection, draft preparation All authors have read and agreed with the manuscript before its submission and publication.

Funding

This research received no specific financial support from any funding agency.

Institutional Review Board Statement

Not applicable.

References

[1] Fan, Y., Xiao, F., Li, C., Yang, G., & Tang, X. (2020). A novel deep learning framework for state of health estimation of lithium-ion battery. Journal of Energy Storage, 32, 101741. https://doi.org/10.1016/j.est.2020.101741

[2] Li, W., Rentemeister, M., Badeda, J., Jöst, D., Schulte, D., & Sauer, D. U. (2020). Digital twin for battery systems: Cloud battery management system with online state-of-charge and state-of-health estimation. Journal of Energy Storage, 30, 101557. https://doi.org/10.1016/j.est.2020.101557

[3] Gong, X., Wang, D., & Cheng, P. (2022). An encoder-decoder model based on deep learning for state of health estimation of lithium-ion battery. Journal of Energy Storage, 46, 103804. https://doi.org/10.1016/j.est.2021.103804

[4] Hossain Lipu, M. S., Ansari, S., Miah, M. S., Meraj, S. T., Hasan, K., & Hussain, A. (2022). Deep learning enabled state of charge, state of health and remaining useful life estimation for smart battery management system: Methods, implementations, issues and prospects. Journal of Energy Storage, 55, 105752. https://doi.org/10.1016/j.est.2022.105752

[5] Kim, T., Krüger, L., & Kowal, J. (2020). On-line state-of-health estimation of lithium-ion battery cells using frequency excitation. Journal of Energy Storage, 32, 101841. https://doi.org/10.1016/j.est.2020.101841

[6] Sui, X., He, S., Vilsen, S. B., Meng, J., Teodorescu, R., & Stroe, D. I. (2021). A review of non-probabilistic machine learning-based state of health estimation techniques for lithium-ion battery. Applied Energy, 300, 117346. https://doi.org/10.1016/j.apenergy.2021.117346

[7] Wang, Y., Song, D., Yuan, W., & Li, R. (2021). A flexible method for state-of-health estimation of lithium battery energy storage system. Energy Reports, 7, 6375-6383. https://doi.org/10.1016/j.egyr.2021.09.054

[8] Meng, J., Cai, L., Stroe, D. I., Ma, J., Luo, G., & Teodorescu, R. (2020). An optimized ensemble learning framework for lithium-ion battery state of health estimation in energy storage system. Energy, 206, 118140. https://doi.org/10.1016/j.energy.2020.118140

[9] Song, Y., Zhang, Y., Liang, J., & Han, X. (2020). Intelligent state of health estimation for lithium-ion battery pack based on big data analysis. Journal of Energy Storage, 32, 101836. https://doi.org/10.1016/j.est.2020.101836

[10] Liu, Z., Li, H., Yao, D., & Wang, Y. (2022). Research on battery SOH estimation algorithm of energy storage frequency modulation system. Energy Reports, 8, 217-223. https://doi.org/10.1016/j.egyr.2021.11.015

[11] Pradhan, S. K., & Chakraborty, B. (2022). Battery management strategies: An essential review for battery state of health monitoring techniques. Journal of Energy Storage, 51, 104427. https://doi.org/10.1016/j.est.2022.104427

[12] Choi, Y. (2020). A study on state of charge and state of health estimation in consideration of lithium-ion battery aging. Sustainability, 12(24), 10451. https://doi.org/10.3390/su122410451

[13] Sugiyama, K., Fujita, T., & Morita, H. (2021). Estimation of cell balance and degradation of individual cells for a multi-cell battery pack connected in series by Charging Curve Analysis Method. Denki Kagaku, 89(2), 101-106. https://doi.org/10.5796/denkikagaku.21-fe0011

[14] Naguib, M., Kollmeyer, P., & Emadi, A. (2021). Lithium-ion battery pack robust state of charge estimation, cell inconsistency, and balancing: Review. IEEE Access, 9, 50570-50582. https://doi.org/10.1109/access.2021.3068776

[15] Dong, G., Huang, M., & Zhao, X. (2021). Low complexity state-of-charge estimation for lithium-ion battery pack considering cell inconsistency. Journal of Power Sources, 515, 230599. https://doi.org/10.1016/j.jpowsour.2021.230599

[16] Reddy, K. J., Routh, P. S., Patra, A., & Mukhopadhyay, S. (2021). Gaussian process regression-based state of health estimation of lithium-ion batteries using indirect battery health indicators. 2021 IEEE International Conference on Prognostics and Health Management, 1-7. https://doi.org/10.1109/icphm51084.2021.9486519

[17] He, W., Bian, X., Liu, L., Wei, Z., & Yan, F. (2020). Comparative study of curve determination methods for incremental capacity analysis and state of health estimation of lithium-ion battery. Journal of Energy Storage, 29, 101400. https://doi.org/10.1016/j.est.2020.101400

[18] Zhou, H., Zhang, S., Peng, J., Zhang, S., Li, J., Xiong, H., et al. (2021). Informer: Beyond efficient Transformer for long sequence time-series forecasting. Proceedings of the AAAI Conference on Artificial Intelligence, 35(12), 11106-11115. https://doi.org/10.1609/aaai.v35i12.17325

[19] Sun, X., Chen, X., Qin, Y., & Wang, Y. (2022). Multi-step time series forecasting based on Informer-XGBoost-GA. Journal of Physics: Conference Series, 2333(1), 012009. https://doi.org/10.1088/1742-6596/2333/1/012009

[20] Ke, S., Zhou, X., Zhu, H., & Peng, Y. (2021). State of health estimation of lithium-ion battery with uncertainty quantification based on Bayesian deep learning. 2021 3rd International Conference on System Reliability and Safety Engineering, 12-18. https://doi.org/10.1109/srse54209.2021.00009

[21] Hong, J., Lee, D., Jeong, E. R., & Yi, Y. (2020). Towards the swift prediction of the remaining useful life of lithium-ion batteries with end-to-end deep learning. Applied Energy, 278, 115646. https://doi.org/10.1016/j.apenergy.2020.115646

[22] Gao, Y., Li, X., & Huang, Y. (2022). An improved deep extreme learning machine to predict the remaining useful life of lithium-ion battery. Frontiers in Energy Research, 10, 1032660. https://doi.org/10.3389/fenrg.2022.1032660

[23] Shen, S., Zhou, M., Wang, C., & Wang, Q. (2022). State of charge estimation for lithium-ion battery using Transformer with immersion and invariance adaptive observer. Journal of Energy Storage, 45, 103768. https://doi.org/10.1016/j.est.2021.103768

[24] Choi, J., Choi, S., & Whangbo, T. (2022). Design and development of a battery state of health estimation model for efficient battery monitoring systems. Sensors, 22(12), 4444. https://doi.org/10.3390/s22124444

[25] Liu, K., He, Y., Bian, X., Guo, Y., & Zhang, X. (2022). A review of lithium-ion battery state of charge estimation based on deep learning: Directions for improvement and future trends. Journal of Energy Storage, 52, 104664. https://doi.org/10.1016/j.est.2022.104664

[26] Park, S., Zhang, Z., Klein, R., & Moura, S. (2021). Estimation of cyclable lithium for Li-ion battery state-of-health monitoring. 2021 American Control Conference, 3094-3101. https://doi.org/10.23919/acc50511.2021.9482841

[27] Bezha, M., Nanahara, T., & Nagaoka, N. (2021). Development of fast SoH estimation of Li-ion battery pack/modules using multi series-parallel based ANN structure. 2021 IEEE 12th Energy Conversion Congress & Exposition - Asia, 1719-1724. https://doi.org/10.1109/ecce-asia49820.2021.9479414

[28] Wu, J., Xu, Y., Jiang, J., & Li, X. (2021). Abnormal battery location recognition and state estimation in lithium battery pack. 2021 33rd Chinese Control and Decision Conference, 6719-6724. https://doi.org/10.1109/ccdc52312.2021.9601743

[29] Wang, Y., Guo, J., & Guo, L. (2022). A hybrid state of health estimation method for lithium-ion battery. 2022 4th International Conference on Data-driven Optimization of Complex Systems, 1-6. https://doi.org/10.1109/docs55193.2022.9967726

[30] Karmawijaya, A., Haq, I. N., Leksono, E., & Widyotriatmo, A. (2022). Development of Remaining Useful Life (RUL) Prediction of Lithium-ion Battery Using Genetic Algorithm-Deep Learning Neural Network (GADNN) Hybrid Model. 2022 7th International Conference on Electric Vehicular Technology, 13-19. https://doi.org/10.1109/icevt55516.2022.9924776

[31] Xiong, R. (2020). Battery SOC and SOH estimation. Battery Management Algorithm for Electric Vehicles, 107-165. https://doi.org/10.1007/978-981-15-0248-4_4

[32] Zhang, Y., Zeng, X., Chang, Y., & Wang, H. (2022). Lithium-ion battery state of health estimation based on improved deep extreme learning machine. Journal of Electrochemical Energy Conversion and Storage, 19(3), 030904. https://doi.org/10.1115/1.4052535

[33] Jeewandara, D., JP, K., & Hemapala, K. (2021). SOC level estimation of lithium-ion battery based on time series forecasting algorithms for battery management system. 2021 3rd International Conference on Electrical Engineering, 43-49. https://doi.org/10.1109/eecon52960.2021.9580869

[34] Jiao, R., Ma, Y., Li, X., & Xiao, M. (2022). Battery remaining useful life prediction based on a combination of ARMA and degradation model. 2022 13th International Conference on Reliability, Maintainability, and Safety, 115-119. https://doi.org/10.1109/icrms55680.2022.9944596

[35] Li, W., Ma, H., Wu, T., & Cheng, C. (2020). State of health equalization strategy for retired battery-based energy storage system. 2020 IEEE 4th Conference on Energy Internet and Energy System Integration, 392-397. https://doi.org/10.1109/ei250167.2020.9346952

[36] He, H., Jin, X., Hu, X., & Li, Y. (2022). Efficient estimation method for state of charge of multi-cell battery pack considering cell inconsistency. International Journal of Electrochemical Science, 17(8), 220827. https://doi.org/10.20964/2022.08.43

[37] Yang, F., Wei, Z., Fang, K., & Dai, H. (2019). SOC estimation of battery pack considering cell inconsistency. SAE Technical Paper Series, 1, 2019-01-1309. https://doi.org/10.4271/2019-01-1309

[38] Zou, Y., Song, X., & Yan, F. (2022). Lithium-ion battery remaining useful life prediction based on hybrid model. 2022 7th International Conference on Intelligent Computing and Signal Processing, 714-719. https://doi.org/10.1109/icsp54964.2022.9778611

[39] Hou, J., Qu, M., Yang, Y., & Su, L. (2022). Remaining useful life prediction of lithium-ion battery based on dual particle filter. 2022 China Automation Congress, 5374-5379. https://doi.org/10.1109/cac57257.2022.10055725

[40] Gou, B., Xu, Y., Fang, S., & Pratama, M. (2019). Remaining useful life prediction for lithium-ion battery using ensemble learning method. 2019 IEEE Power & Energy Society General Meeting, 1-5. https://doi.org/10.1109/pesgm40551.2019.8973811